

Muon-spin rotation and relaxation study on the quasi-one-dimensional compounds $\text{Ca}_3\text{CoRhO}_6$, $\text{Sr}_4\text{CoRh}_2\text{O}_9$, and $\text{Sr}_5\text{CoRh}_3\text{O}_{12}$

Jun Sugiyama,^{1,*} Hiroshi Nozaki,¹ Yutaka Ikeda,¹ Peter L. Russo,² Kazuhiko Mukai,¹ Daniel Andreica,³ Alex Amato,³ Tsuyoshi Takami,⁴ and Hiroshi Ikuta⁴

¹Toyota Central Research and Development Labs. Inc., Nagakute, Aichi 480-1192, Japan

²TRIUMF, 4004 Wesbrook Mall, Vancouver, British Columbia, V6T 2A3 Canada

³Laboratory for Muon Spin Spectroscopy, Paul Scherrer Institut, CH-5232 Villigen PSI, Switzerland

⁴Department of Crystalline Materials Science, Nagoya University, Furo-cho, Chikusa-ku, Nagoya, 464-8603 Japan

(Received 18 December 2007; published 18 March 2008)

Thanks to the unique power of muon-spin spectroscopy, we found that the quasi-one-dimensional Co-Rh oxides $A_{n+2}\text{CoRh}_n\text{O}_{3n+3}$ ($A=\text{Ca}, \text{Sr}$; $n=1, 2$, and 3) exhibit a two-dimensional antiferromagnetic transition that ranges from $T_N^{\text{on}}=185$ K for $n=1$ to 125 K for $n=3$ with a transition width (ΔT) of about 80 K. The variation of T_N^{on} with n is explained by the increase in the distance between the neighboring $\text{CoRh}_n\text{O}_{3n+3}$ chains. Static magnetic order is observed below the end point of T_N ($=T_N^{\text{on}}-\Delta T$) for each of the three samples. The existence of the two-frequency components in the zero field spectrum indicates the appearance of ferrimagnetic order for $\text{Ca}_3\text{CoRhO}_6$ below 20 K.

DOI: 10.1103/PhysRevB.77.092409

PACS number(s): 75.30.Kz, 76.75.+i, 75.25.+z

Dimensionality of real compounds is not determined straightforwardly from their crystal structure. Indeed, in spite of the one-dimensional (1D) structural nature of the quasi-1D (Q1D) cobalt oxides $A_{n+2}\text{Co}_{n+1}\text{O}_{3n+3}$ ($A=\text{Ca}, \text{Sr}$, and Ba with $n=1-5$, and ∞), a two-dimensional (2D) antiferromagnetic (AF) transition has been clearly detected below 100 K exclusively by a positive muon-spin rotation and relaxation ($\mu^+\text{SR}$) technique.¹ The 2D magnetic nature has also been confirmed by high-pressure $\mu^+\text{SR}$ experiments.² Noting that the connections between the CoO_3 chains form a 2D triangular lattice in the c plane of the Q1D lattice, the CoO_3 chain in the $n=1$ compound consists of alternating face-sharing CoO_6 trigonal prisms and CoO_6 octahedra.^{3,4} As n increases, only the number of CoO_6 octahedra increases so as to build the chain with n CoO_6 octahedra and one CoO_6 trigonal prism.^{5,6} The magnetic interaction is ferromagnetic (FM) along the CoO_3 chain (1D-FM) and AF in the 2D triangular lattices (2D-AF). The Q1D cobalt oxides are therefore thought to be 2D antiferromagnets with FM Ising-spin chains.

Combining the result of recent susceptibility measurements⁷ with past work,^{1,2} a sequence of successive magnetic transitions of $\text{Ca}_3\text{Co}_2\text{O}_6$ ($n=1$) was clarified as follows: as T decreases from ambient temperature, 1D-FM order, probably short range, appears below ~ 150 K (T_C^{SR}), then short-range 2D-AF order appears below 100 K (T_N^{SR}) [the 2D-AF order completes below ~ 25 K (T_N)], and finally, $\text{Ca}_3\text{Co}_2\text{O}_6$ enters into a ferrimagnetic state below 15 K (T_{ferri}). Here, a coherent precession in the zero field (ZF) $\mu^+\text{SR}$ spectrum means that all the muons feel the same internal field, indicating the formation of long-range order. On the contrary, a fast relaxing signal without precession suggests wide field distribution at the muon sites, implying the appearance of short-range order. For the Q1D cobalt oxides with $n=2-5$, although the long-range order never completes even down to 1.8 K, i.e., T_N and T_{ferri} are never reached, the rest of the sequence is essentially the same as that of $\text{Ca}_3\text{Co}_2\text{O}_6$. It is also found that the onset temperature

($T_N^{\text{on}}=T_N^{\text{SR}}$) decreases with increasing n due to the increase in the interchain distance. On the other hand, the other end member BaCoO_3 ($n=\infty$) exhibits two magnetic transitions;^{1,8} one is a short-range FM transition with $T_C^{\text{SR}}=53$ K and the other an AF transition, an amplitude modulated AF phase, with $T_N=15$ K.⁹

The complex magnetic behavior of the Q1D cobalt oxides is caused by competition between the 1D-FM and 2D-AF interactions. This leads to the question of how the magnetic structure changes if the balance between the two interactions is changed by elemental substitutions. Fortunately, the Co ions in the CoO_6 octahedron can be fully substituted by other elements in $\text{Ca}_3\text{Co}_2\text{O}_6$; that is, Ca_3CoMO_6 with $M=\text{Sc}, \text{Rh}, \text{Ru}$, and Ir were successfully prepared.^{10,11} For the $M=\text{Rh}$ case, since the Weiss temperature (Θ_p) of $\text{Ca}_3\text{CoRhO}_6$ is about 150 K but that of $\text{Ca}_3\text{Co}_2\text{O}_6$ is 30 K, the Rh substitution clearly enhances the 1D-FM interaction. Nevertheless, a recent neutron diffraction (ND) study¹² has revealed the existence of two types of 2D-AF order. That is, a partially disordered antiferromagnetic (PDA) state,¹³ in which two-thirds of the chains are coupled antiferromagnetically, but the remaining third stays incoherent, appears below 90 K, and then the PDA state apparently freezes below 30 K, i.e., a frozen PDA (FPDA) state.¹² There is, however, no information on short-range 2D-AF order in $\text{Ca}_3\text{CoRhO}_6$ by ND measurements, as in the case of the pure Q1D cobalt oxides. Very recently, not only $\text{Ca}_3\text{CoRhO}_6$ ($n=1$) but also $\text{Sr}_4\text{CoRh}_2\text{O}_9$ ($n=2$) and $\text{Sr}_5\text{CoRh}_3\text{O}_{12}$ ($n=3$) were prepared,¹⁴ although the magnetic behavior of the latter two compounds has been investigated even less. In what follows, we call these compounds Rh-Q1D.

In this Brief Report, we report a study of the microscopic magnetic nature of the Rh-Q1D compounds with $n=1-3$ by means of $\mu^+\text{SR}$, which is very sensitive to the local magnetic and structural environments, because the implanted μ^+ 's experience the magnetic field generated mainly by their nearest neighbors. We clearly demonstrate the appearance of short-range 2D-AF order for the Rh-Q1Ds, similar to the Q1D

cobalt oxides.^{1,2} We propose that the short-range 2D-AF order is common to the Q1D systems with FM Ising-spin chains, although the predominant element in the 1D chains changes from Co to Rh. Furthermore, ZF- μ^+ SR measurements down to 20 mK suggest that the magnetic order of $\text{Ca}_3\text{CoRhO}_6$ below 20 K is not an FPDA but ferrimagnetic, in contrast to the ND results.¹²

Polycrystalline samples of $\text{Ca}_3\text{CoRhO}_6$ ($n=1$), $\text{Sr}_4\text{CoRh}_2\text{O}_9$ ($n=2$), and $\text{Sr}_5\text{CoRh}_3\text{O}_{12}$ ($n=3$) were synthesized at Nagoya University by a conventional solid state reaction technique, using reagent grade Co_3O_4 , CaCO_3 , SrCO_3 , and Rh powders as starting materials. Powder x-ray diffraction experiments were performed to check the purity and the crystal structure. Magnetic susceptibility (χ) was measured using a superconducting quantum interference device magnetometer (MPMS, Quantum Design) with T ranging between 2 and 300 K and a magnetic field $H=10$ kOe. The preparation and characterization of the Rh-Q1D samples with $n=1-3$ were reported in detail elsewhere.¹⁴ The μ^+ SR experiments were performed on the $\pi\text{E1-Dolly}$ and the $\pi\text{M3-LTF}$ surface muon beam lines at PSI, using an experimental setup and techniques described elsewhere.¹⁵

Figure 1 confirms the existence of a magnetic transition with T_N^{on} of ~ 185 K for the $n=1$, ~ 130 K for the $n=2$, and ~ 125 K for the $n=3$ sample, because the weak transverse field (wTF) asymmetry (A_{TF}) is roughly proportional to the volume fraction of paramagnetic phases in the sample. The accompanying increase in the relaxation rate (λ_{TF}) shows the appearance of internal magnetic fields (H_{int}), which are larger than the applied wTF (50 Oe in this case). Although the transition width (ΔT) ranges from 60 to 80 K due to the 2D nature and geometrical frustration of the triangular lattice, the wTF asymmetry reaches almost 0 below T_N^{end} ($=T_N^{\text{on}}-\Delta T$) for all cases, meaning that the whole sample is in the magnetic state below T_N^{end} . Note that χ and ND experiments provided no information on T_N^{on} , but they gave clear anomalies for the $n=1$ compound only below 90 K ($=T_N^{\text{end}}$),¹² at which the transition completes from the viewpoint of wTF- μ^+ SR.

The decrease in T_N^{on} with n is explained by the increase in the interchain distance (d_{ic}), as for the pure Q1D cobalt oxides [see Fig. 1(d)].² Since the interchain interaction is naturally enhanced with decreasing d_{ic} , this is most likely to support the 2D nature of the transition detected by wTF- μ^+ SR. Making a comparison with the $T_N^{\text{on}}(d_{\text{ic}})$ curve for the Q1D's, the curve for the Rh-Q1D's is shifted by ~ 80 K towards higher T . This is consistent with the fact that the $4d$ orbitals of Rh are more widely spread out than the $3d$ orbitals of Co.

In order to investigate the magnetic nature below T_N^{end} , we measured the ZF spectrum down to 20 mK. For all three samples, the ZF spectrum shows a fast relaxation and a first minimum below $\sim 0.05 \mu\text{s}$ at 20 mK (see Fig. 2). Only for the $n=1$ sample does the ZF spectrum exhibit two minima, indicating formation of static (at least for muon's lifetime, 2.2 μs) order. More precisely, there are two different frequency components. Although the top two spectra seem to be typical for Kubo-Toyabe-type relaxation due to dense randomly oriented moments,¹⁵ a strongly damped cosine oscillation due to static order with wide field distribution is more

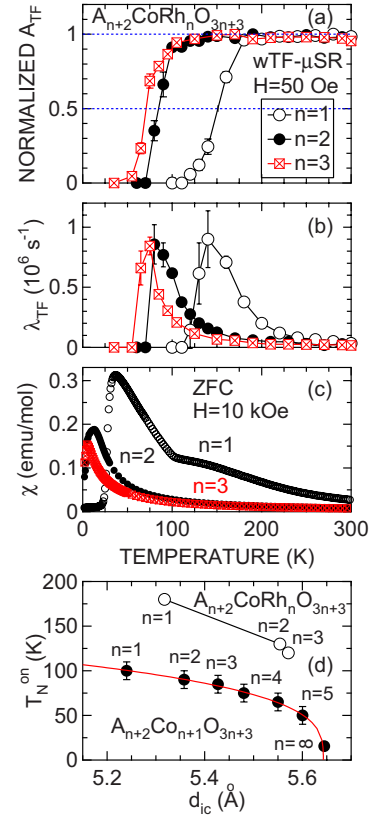


FIG. 1. (Color online) T dependences of (a) normalized wTF asymmetry, (b) relaxation rate, (c) χ for $A_{n+2}\text{CoRh}_n\text{O}_{3n+3}$,¹⁴ and (d) the relationship between T_N^{end} and the interchain distance (d_{ic}) for the Rh-Q1D's and pure Q1D cobalt oxides.² The μ^+ SR data was obtained by fitting the wTF spectrum using an exponential relaxed cosine oscillation function, $A_{\text{TF}} \exp(-\lambda_{\text{TF}}t) \cos(\omega_{\mu}t + \phi)$. χ was measured in the magnetic field of $H=10$ kOe in zero field cooling mode. Relatively large error bars in (b) especially for the $n=1$ sample are caused by the abrupt decrease in A_{TF} [see (a)].

suitable for fitting the spectrum, especially for explaining the fast relaxing behavior in the early time domain (below 0.02–0.04 μs). We therefore fitted the ZF- μ^+ SR spectra with the following function:

$$A_0 P_{\text{ZF}}(t) = A_{\text{AF1}} e^{-\lambda_1 t} \cos(\omega_{\mu 1} t + \phi) + A_{\text{AF2}} e^{-\lambda_2 t} \cos(\omega_{\mu 2} t + \phi) + A_{\text{fast}} e^{-\lambda_{\text{fast}} t} + A_{\text{tail}} e^{-\lambda_{\text{tail}} t}, \quad (1)$$

where the second term is used instead of the third term only for the $n=1$ sample below 20 K. The A_{fast} term, which gives only minor contributions (below 7%), is caused by fluctuating moments at the disordered sites, while the A_{tail} corresponds to the “1/3 tail” caused by the AF field component parallel to the initial muon-spin polarization.

Figure 3 shows the T dependences of the muon precession frequencies ($f_i = \omega_{\mu i} / 2\pi$) and their normalized asymmetries ($A_{\text{AF}i}$) for the three samples. Both f and A_{AF} have finite values below 95 K for the $n=1$, 55 K for the $n=2$, and 43 K for the $n=3$ sample, respectively. The magnitude of $f(T \rightarrow 0 \text{ K})$ for the three samples is roughly the same (~ 10 MHz), suggesting that the internal field along the Ising-type chain is independent of n . This is because the μ^+ 's naturally locate at

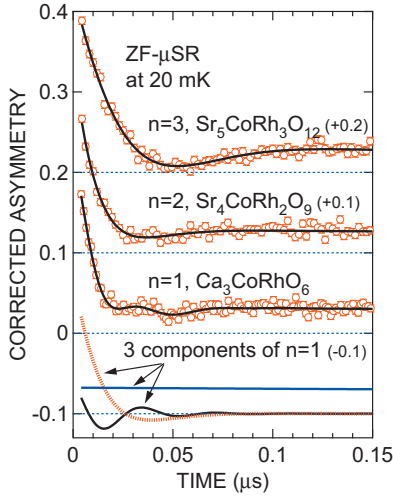


FIG. 2. (Color) ZF- μ^+ SR spectrum of $A_{n+2}\text{CoRh}_n\text{O}_{3n+3}$ at 20 mK. Each spectrum is offset by 0.1 for clarity of display. Solid lines represent the fitting result using Eq. (1); the bottom three lines represent three components for the $n=1$ sample.

the vicinity of O^{2-} ions in the chain. Note that an additional high-frequency component appears only for the $n=1$ sample below 20 K, around which the $\chi_{\text{ZFC}}(T)$ curve exhibits a maximum and neutron scattering suggests the presence of frozen PDA order.¹² The normalized $A_{\text{AF}}(T)$ curves show that the majority of each sample ($\sim 90\%$) enters into the AF phase below T_N^{end} , at which the static internal field appears.

Since neutron measurements showed the existence of a PDA state below ~ 90 K for $\text{Ca}_3\text{CoRhO}_6$, the first AF component with $f_1 \sim 10$ MHz naturally corresponds to the internal field of the PDA state. Actually, assuming that there are only two μ^+ sites in the lattice [see Fig. 4(a)] because of the absence of a structural phase transition down to 2 K, a dipole field calculation gives that the overall distribution of the

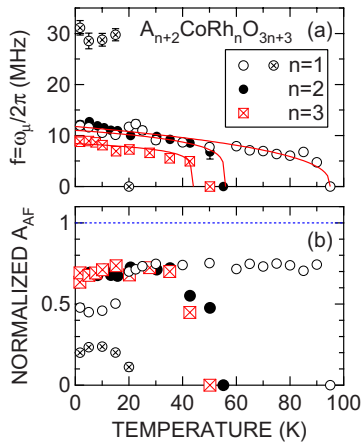


FIG. 3. (Color online) T dependences of (a) oscillation frequency $f \equiv \omega_\mu/2\pi$ and (b) normalized asymmetry of the oscillatory component for $A_{n+2}\text{CoRh}_n\text{O}_{3n+3}$. In (a), solid lines represent the fitting result using the equation $f/f_0 = [(T_N - T)/T_N]^\beta$; since $\beta = 0.212$ for $n=1$, 0.184 for $n=2$, and 0.135 for $n=3$, Rh-Q1D's are likely to approach the ideal 2D-Ising model ($\beta = 1/8$) with increasing n .

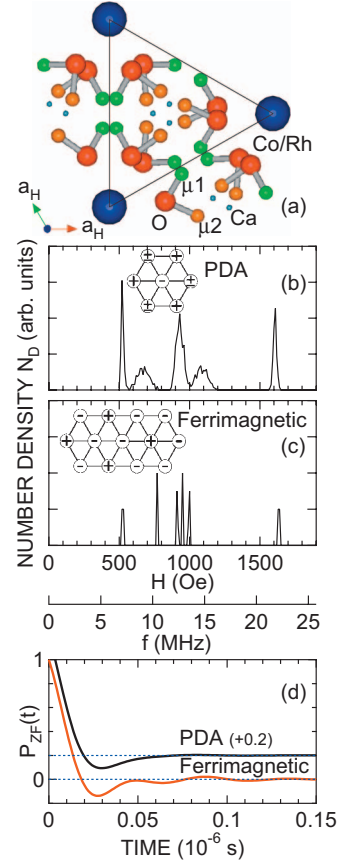


FIG. 4. (Color) (a) Two muon sites ($\mu 1$ and $\mu 2$) proposed by electrostatic potential calculations in the $\text{Ca}_3\text{CoRhO}_6$ lattice, dipolar field distribution (N_D) for (b) the PDA and FPDA and (c) ferrimagnetic state, and (d) the muon-spin polarization function in ZF [$P_{\text{ZF}}(t)$] predicted for both states. N_D was obtained by dipole sum calculations for the two muon sites using the magnetic moment $3\mu_B$ of Co^{2+} and $1\mu_B$ of Rh^{4+} ,^{12,16} both calculations were performed by the program DipElec.¹⁷ Since the ratio of up and down spin is 0.5 for the ferrimagnetic state in (c), it is not a simple AF. $P_{\text{ZF}}(t)$ was calculated by $\exp(-\lambda t) \sum N_{D,i} \cos(2\pi f_i t)$, where $\lambda_{\text{PDA}} = \lambda_{\text{ferri,lf}} = 50 \times 10^6 \text{ s}^{-1}$ and $\lambda_{\text{ferri,hf}} = 25 \times 10^6 \text{ s}^{-1}$ due to the difference of the full width at half maximum for the hf component between the PDA and ferrimagnetic state; here, hf and lf stand for the high field (~ 1600 Oe) and low field (below 1200 Oe) components, respectively.

PDA state is centered at 13 MHz with a standard deviation of 5 MHz [see the top spectrum in Fig. 4(d)], although there are several f components as seen in Fig. 4(b). This is consistent with the strongly damped cosine oscillation observed between 20 and 95 K.

In order to explain the appearance of the second AF component, another magnetically ordered state should thus appear below 20 K. Considering the coexistence of the two AF components, the following two states are reasonably acceptable, that is, a ferrimagnetic state and a frozen PDA (FPDA) state. Figure 4(c) shows the field distribution for the ferrimagnetic state derived from the PDA state; that is, incoherent chains align ferromagnetically along the c axis. Since the two sites are clearly distinguishable below 20 K, a possible magnetic order below 20 K is the ferrimagnetic state [see the

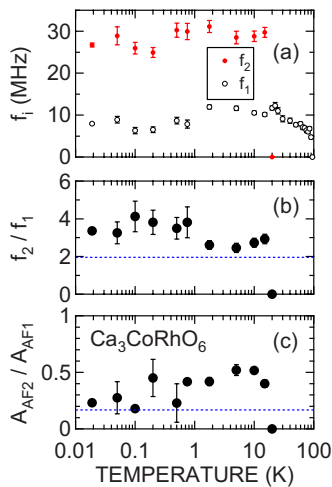


FIG. 5. (Color online) T dependences of (a) the two oscillation frequencies (f_1 and f_2), (b) the ratio of the frequencies (f_2/f_1), and (c) the ratio of the asymmetries (A_{AF2}/A_{AF1}) for $\text{Ca}_3\text{CoRhO}_6$. The broken lines in (b) and (c) represent the prediction for the ferrimagnetic state (see Fig. 4). The data above 1 K is also plotted in Fig. 3 in a linear T scale.

bottom spectrum in Fig. 4(d)], because the field distribution of the FPDA state is essentially the same as that of the PDA state, for which only one frequency is seen. A simple dipole field calculation yields a ratio of 1.95 for the two frequencies, and 1/6 for the number density of the two frequencies.

Both ratios are in reasonable agreement with the current μ^+ SR result particularly below 0.5 K (see Fig. 5).

In summary, it is clarified that $\text{Ca}_3\text{CoRhO}_6$ undergoes successive transitions from a high- T paramagnetic state to a short-range AF state at 185 K ($=T_N^{\text{SR}}=T_N^{\text{on}}$), to a PDA state at ~ 90 K ($=T_N^{\text{LR}}=T_N^{\text{end}}$), and then to a ferrimagnetic structure below 20 K ($=T_{\text{ferri}}$). For the other two Rh-Q1D's, $T_N^{\text{SR}}=130$ K and $T_N^{\text{LR}}=55$ K for $n=2$ (125 K and 43 K for $n=3$), but they never enter into the ferrimagnetic state even down to 20 mK. Finally, we wish to remark on the significance of the Ising-type FM nature of the Q1D system. Since T_N^{on} ranges from 185 to 125 K, the 1D-FM transition temperature is naturally expected to be equal or above T_N^{on} . In particular, both orders could occur simultaneously for the Rh-Q1D's, because $\Theta_p (=150$ K) is comparable to T_N^{on} . In order to detect 1D-FM order, it is necessary to perform inelastic neutron experiments using a single crystal sample.

ACKNOWLEDGMENTS

This work was performed at the Swiss Muon Source, Paul Scherrer Institut, Villigen, Switzerland. We thank the staff of PSI for help with the μ^+ SR experiments. Y.I., H.N., and J.S. are partially supported by the KEK-MSL Inter-University Program for Oversea Muon Facilities. T.T. is supported by the JSPS Research Fellowships for Young Scientists. This work is also supported by Grant-in-Aid for Scientific Research (B), 19340107, MEXT, Japan.

*e0589@mosk.tytlabs.co.jp

- ¹J. Sugiyama, H. Nozaki, J. H. Brewer, E. J. Ansaldo, T. Takami, H. Ikuta, and U. Mizutani, Phys. Rev. B **72**, 064418 (2005).
- ²J. Sugiyama, H. Nozaki, Y. Ikeda, K. Mukai, D. Andreica, A. Amato, J. H. Brewer, E. J. Ansaldo, G. D. Morris, T. Takami, and H. Ikuta, Phys. Rev. Lett. **96**, 197206 (2006).
- ³H. Fjellvåg, E. Gulbrandsen, S. Aasland, A. Olsen, and B. C. Hauback, J. Solid State Chem. **124**, 190 (1996).
- ⁴S. Aasland, H. Fjellvåg, and B. Hauback, Solid State Commun. **101**, 187 (1997).
- ⁵K. Boulahya, M. Parras, and J. M. González-Calbet, J. Solid State Chem. **142**, 419 (1999).
- ⁶M.-H. Wangbo, H.-J. Koo, K.-S. Lee, O. Gourdon, M. Evain, S. Jobic, and R. Brec, J. Solid State Chem. **160**, 239 (2001).
- ⁷T. Takami, H. Nozaki, J. Sugiyama, T. Takeuchi, and H. Ikuta, J. Magn. Magn. Mater. **310**, 438 (2007).
- ⁸K. Yamaura, H. W. Zandbergen, K. Abe, and R. J. Cava, J. Solid State Chem. **146**, 96 (1999).
- ⁹H. Nozaki, M. Janoschek, B. Roessli, J. Sugiyama, L. Keller, J. H. Brewer, E. J. Ansaldo, G. D. Morris, T. Takami, and H. Ikuta, Phys. Rev. B **76**, 014402 (2007).
- ¹⁰H. Kageyama, K. Yoshimura, and K. Kosuge, J. Solid State Chem. **140**, 14 (1998).
- ¹¹A. Maignan, S. Hébert, C. Martin, and D. Flahaut, Mater. Sci. Eng., B **104**, 121 (2003).
- ¹²S. Niitaka, K. Yoshimura, K. Kosuge, M. Nishi, and K. Kakurai, Phys. Rev. Lett. **87**, 177202 (2001).
- ¹³M. Mekata, J. Phys. Soc. Jpn. **42**, 76 (1977).
- ¹⁴T. Takami and H. Ikuta, J. Appl. Phys. **103**, 07B701 (2008).
- ¹⁵G. M. Kalvius, D. R. Noakes, and O. Hartmann, in *Handbook on the Physics and Chemistry of Rare Earths*, edited by K. A. Gschneidner Jr. et al. (North-Holland, Amsterdam, 2001), Vol. 32, pp. 55–51, and references cited therein.
- ¹⁶K. Takubo, T. Mizokawa, S. Hirata, J.-Y. Son, A. Fujimori, D. Topwal, D. D. Sarma, S. Rayaprol, and E.-V. Sampathkumaran, Phys. Rev. B **71**, 073406 (2005).
- ¹⁷K. M. Kojima, J. Yamanobe, H. Eisaki, S. Uchida, Y. Fudamoto, I. M. Gat, M. I. Larkin, A. Savici, Y. J. Uemura, P. P. Kyriakou, M. T. Rovers, and G. M. Luke, Phys. Rev. B **70**, 094402 (2004).